Journal of Electroanalytical Chemistry 657 (2011) 107–112

Contents lists available at ScienceDirect

Journal of Electroanalytical Chemistry

journal homepage: www.elsevier.com/locate/jelechem

Electrochemical behavior of antioxidants: I. Mechanistic study on electrochemical oxidation of gallic acid in aqueous solutions at glassy-carbon electrode

Refat Abdel-Hamid *, Emad F. Newair

Department of Chemistry, Faculty of Science, University of Sohag, 82524, Egypt

ARTICLE INFO

Article history:
Received 4 December 2010
Received in revised form 17 March 2011
Accepted 26 March 2011
Available online 6 April 2011

Keywords:
Gallic acid
Cyclic voltammetry
Chronoamperometry
Chronocoulometry
Convolution–deconvolution sweep voltammetry and digital simulation

ABSTRACT

Mechanism of electrochemical oxidation of gallic acid in aqueous phosphate buffer solutions of different pH's was studied at glassy-carbon electrode. The study was performed using cyclic, convolution–deconvolution sweep voltammetry, chronoamperometry and chronocoulometry. It gives two irreversible diffusion-controlled cyclic voltammetric waves at the entire range of pH. The electrochemical oxidation mechanism was proposed to be an ECEC-first order mechanism in which the two electron transfer steps and the two chemical follow-up deprotonation reactions are irreversible. The proposed mechanism was confirmed by digital simulation and the electrode kinetic parameters are estimated on comparing the simulated response with the experimental ones.

1. Introduction

Gallic acid, GA, and its derivatives are a group of naturally occurring polyphenol antioxidants which have recently been shown to have potential health effects [1]. GA is a strong natural antioxidant [2,3]. The acid and its derivatives have a wide range of biological activities, including anti-oxidant, anti-inflammatory, anti-microbial, and anti-cancer activities [4–7]. Electrochemical oxidation of gallic acid has been studied at glassy-carbon electrode [8,9]. It was found that the oxidation process is quasireversible over the studied pH range. An electroanalytical procedure was proposed and applied for determination of gallate content in green tea [8]. The electrochemical oxidation of gallic acid on polyaniline (PAn) and polyaniline-ferrocene phosphonic acid (PAnFc) electrodes was studied by cyclic voltammetry at pH range of 5.0–6.6 [9]. It was found that, the modified electrodes catalyze the oxidation process and are dependent on pH. Furthermore, the PAnFc modified electrode catalyzes better than that of the PAn one.

Antioxidant properties are related with the redox characteristics and consequently, knowledge of the redox behavior is very crucial the antioxidant properties. Antioxidant activity of gallates was studied electrochemically in aqueous media [10].

The electro-oxidation mechanism of gallic acid has been poorly explored in literature. Accordingly, it seems very important to clarify the electrochemical oxidation mechanisms. The objective of the present work is, therefore, to intensively study the electrochemical oxidation of gallic acid in aqueous solutions of different pH's at glassy-carbon electrode. The mechanism is investigated using cyclic, convolution–deconvolution sweep voltammetry, double step chronoamperometry and chronocoulometry and digital simulation under different experimental conditions.

2. Experimental

Gallic acid, GA (99%) was purchased from Sigma–Aldrich. 0.4 M phosphate buffer supporting electrolyte was prepared with various pH values from monosodium phosphate and disodium phosphate in deionized water. Fresh stock standard solution (10 mM) was prepared from the dry pure substances in the phosphate buffer. These solutions were diluted to the convenient concentration just prior to use. All other used solutions were prepared from BHD analytical grade chemicals. A conventional three-electrode electrolytic cell was employed, in which saturated calomel electrode, SCE, a platinum electrode were used as reference and counter electrodes, respectively. Glassy-carbon electrode, GC (surface area = 0.0106 cm^2) was employed as a working electrode. For each voltammetric measurement, the GC working electrode was freshly polished to a smooth surface finish, using successively fine (0.5 μm) grades of

* Corresponding author. Mobile: +20 0183369369; fax: +20 0934601159.
E-mail addresses: Abdelhamid.refat@yahoo.com (R. Abdel-Hamid), newer_emad84@yahoo.com (E.F. Newair).

1572-6657/$ - see front matter © 2011 Elsevier B.V. All rights reserved.
doi:10.1016/j.jelechem.2011.03.030

SiC paper and washed with deionized water. Test solutions were degassed with pure nitrogen prior to the voltammetric measurements. A nitrogen blanket was maintained thereafter. All experiments were performed at room 25 °C temperature. The electrochemical experiments were preformed with an EG & G Princeton Applied Research Model 273A potentiostat controlled by a computer. The electrochemical experiments were controlled by PC and the electrochemical set-up was controlled with an EG & G Princeton Applied Research Model M 270 software. Background data were stored and subtracted from the experimental data set, minimizing side effects such as double layer charging current.

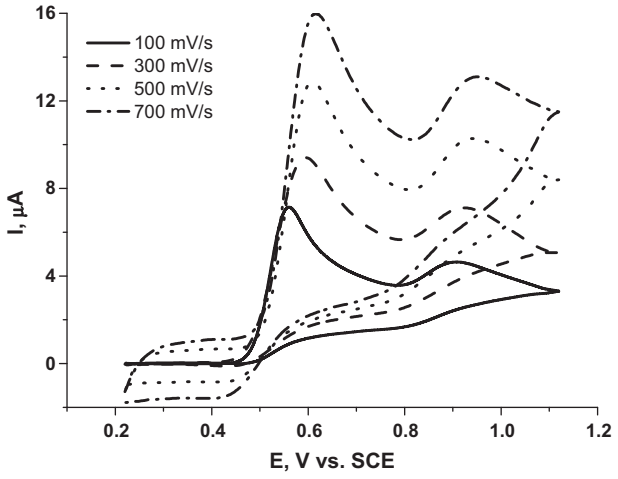

Fig. 1. Cyclic voltammograms of 0.95 mM gallic acid in 0.4 M (pH 1.55) phosphate buffer at different scan rates.

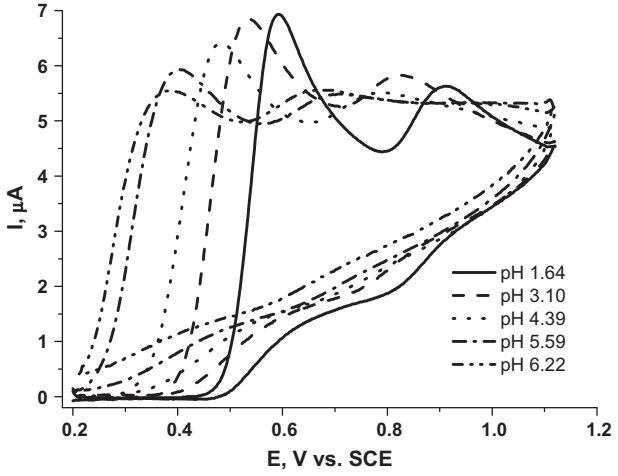

Fig. 2. Cyclic voltammograms of 0.26 mM gallic acid in 0.4 M phosphate buffer with different pH's at scan rate of 100 mV s^{-1}.

For determination of uncompensated resistance, the electrochemical cell is considered electronically equivalent to a RC circuit with the uncompensated resistance, R_u, in series with the double-layer capacitance, C_{dl}. Since faradaic impedance is not considered part of the model, the test potential must be a value at which no faradaic process occurs. A potential step between 25 and −25 mV relative to a test potential is applied and the current is sampled at 50 ms and 100 ms after the step [11]. Assuming the expected exponential decay of the current, characteristic of double layer charging, the initial current, i_o, is determined by extrapolation to zero time. Using Ohm's law, R, is calculated from this measurement as:

$$R_u = \Delta E / i_0 = 50\ \text{mV}/i_0$$

3. Results and discussion

3.1. Cyclic voltammetry

Cyclic voltammograms, cv, of 0.95 mM gallic acid, GA, on glassy-carbon electrode in 0.40 M phosphate buffer at pH 1.55 at different scan rates, v, are shown in Fig. 1. Two irreversible anodic cv waves are seen, their reduction counter-parts are lacking. A linear log–log variation, log peak current, log i_p, versus log scan rate, log v, for both waves is obtained with slope of 0.48 and 0.55 for first and second waves, respectively. Furthermore, the peak current of both waves shows a linear dependence on GA concentration. These results indicate that the two waves are purely diffusion-controlled in nature.

A linear positive shift is observed in the oxidation peak potential, E_p (for the two waves) on increasing scan rate (100–1000 mV s^{-1}). Furthermore, the peak current function, $i_p/v^{1/2}$, diminishes slightly with increasing scan rate. Such behavior is adopted as indicative of an ECEC mechanism [12–14]. On repeated cycling of GA, a decrease of the peak current and a shit of the peak potential towards more positive potentials for the two cv waves are seen with increasing the number of potential cycles during electrolysis (data not shown). This is presumably due to generation of electro-inactive oxidation species on increasing the scanning time. These products block the electrode surface.

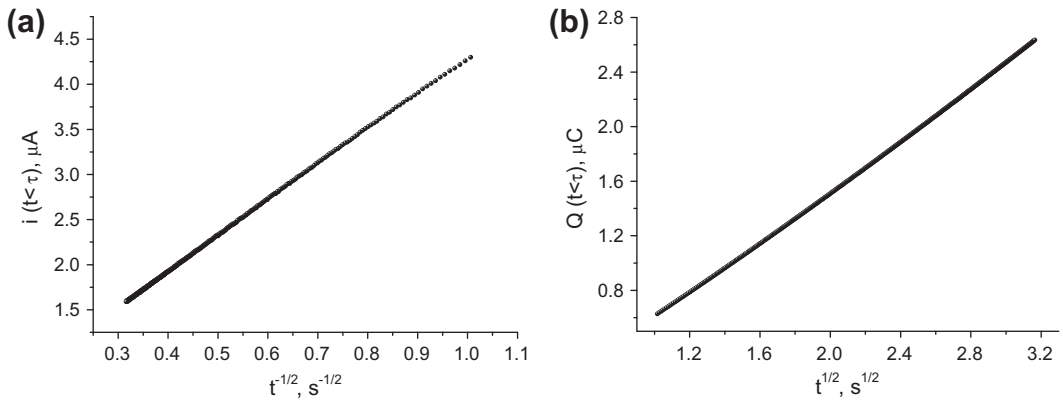

Fig. 3. Chronoamperometry of 0.20 mM gallic acid at pH 1.64, $i(t < \tau)$ versus $(t^{1/2})$ (a) and chronocoulometry, $Q(t < \tau)$ versus $t^{1/2}$ (b).

Fig. 2 shows effect of pH on the voltammetric behavior of gallic acid in aqueous buffer solutions. Two irreversible cv waves are obtained in the whole pH range of study, 1.64–6.22. On increasing pH of solution, the two peak potentials are shifted toward less positive values. The same dependence for oxidation of gallic acid and its derivatives was described elsewhere [8,15,16]. It is generally known that CA is oxidized to quinone via semiquinone form. Thus, a proton (H^+) participates in redox step. A linear least-squares regression lines are obtained for the decrease of E_p as a function of pH for the two cv waves. The regression lines are represented as follows:

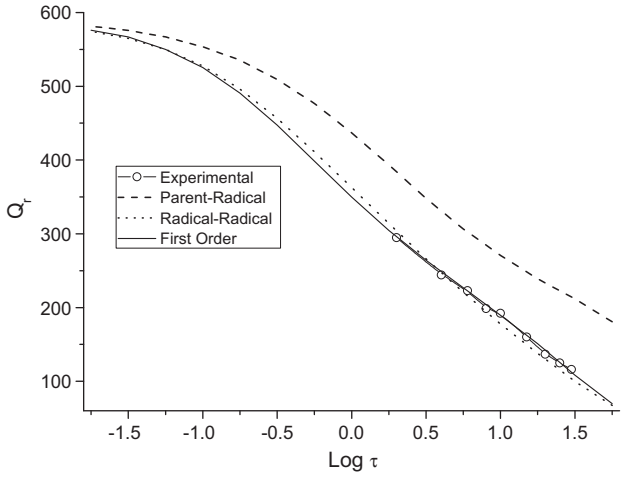

Fig. 4. Best fit of chronocoulometric charge ratio, Q_R for experimental and theoretical working curves for the oxidation ECEC, first-order mechanism of gallic acid.

$$E_p = 682.9 - 47.5\ \text{pH} \quad r = -0.996 \quad \text{for 1st wave} \tag{1}$$

$$E_p = 991.2 - 50.1\ \text{pH} \quad r = -0.994 \quad \text{for 2nd wave} \tag{2}$$

These slopes are in good agreement with the theoretical Nernstian systems with mono-electron transfer step followed by single deprotonation. From Eqs. (1) and (2), the apparent $E^{o\prime}$ for the two waves are 682.9 and 991.2 mV versus SCE, respectively for the first and the second cv waves.

Fig. 2 shows that i_p decreases on increasing pH of the solution. This indicates that the species are gradually deprotonated. On the other hand, in solutions of pH higher than 6.22, the oxidation waves are not observed (data not shown), which indicates that the product of CA oxidation becomes electroinactive and blocks the electrode surface. For this reason the studies are limited to the pH range of 1.64–6.22.

3.2. Convolution–deconvolution sweep voltammetry

Convolution and deconvolution procedures are carried out according to the method described earlier [17]. The convolution current, I_1, is given by the following integration:

$$I_1(t) = \pi^{1/2} \int_0^t \frac{i(t)}{(t-u)^{\frac{1}{2}}} du \tag{3}$$

The deconvolution of current can be expressed as the differential of the I_1 convolution. In more general terms deconvolution is akin to semi-differentiation in a similar manner to considering $t^{-1/2}$ convolution as semi-integration.

The I_1 convolution and deconvolution cyclic voltammograms of gallic acid show a distinct separation between the forward and reverse sweep. This clearly indicates irreversibility of the two

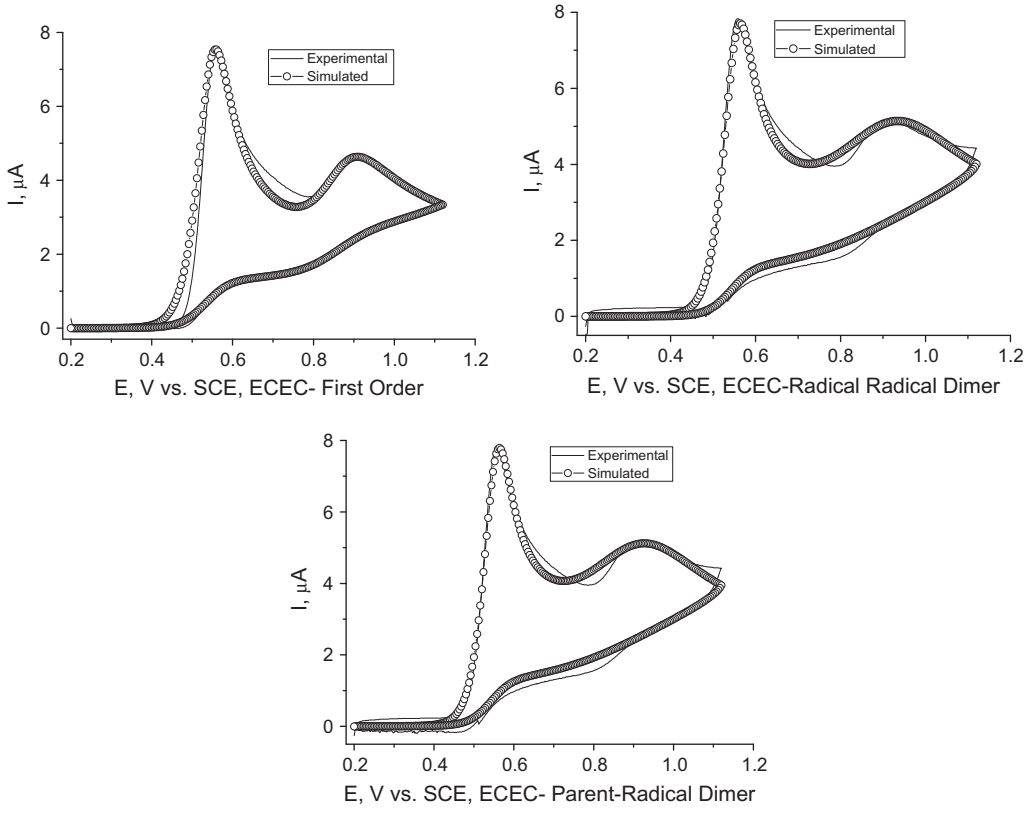

Fig. 5. Best fit of for experimental and digital simulated data for the oxidation mechanisms, ECEC, radical–radical dimer, ECEC, parent-radical dimer and ECEC, first-order of 0.20 mM gallic acid at pH 1.62 and scan rate of 100 mV s^{-1}.

oxidation cv waves. At the entire range of sweep rates, the convoluted current, I_1, neither returns to its initial (zero) value nor superimposed during the reverse half of sweep with I_1 on the forward sweep regardless of the scan rate. This may be due to an irreversible electron transfer process or an electron transfer process coupled with chemical reaction. The diffusion coefficient, D, of the subject substrate can be determined from the limiting value achieved for I_1 when the potential is driven to a sufficiently extreme value past the peak using the following equation [18]:

$$I_{lim} = nFAD^{1/2}C^{bulk} \quad (4)$$

where I_{lim} is the limiting value of current, A is the electrode surface area, C^{bulk} is the bulk concentration of the substrate (mol L^{-1}) and the remaining have their usual meanings. The diffusion coefficient is determined, after applying background subtraction and correction for uncompensated resistance. The diffusion coefficient is calculated to be 4.23×10^{-5} cm^2 s^{-1}.

Deconvolution transformation gives a rapid test for the nature of electron transfer response. Different peak heights in the forward and backward sweeps of deconvoluted current (dI_1/dE) are observed. This gives evidence that the electron transfer process is complicated with a chemical reaction. Furthermore, the estimated values of anodic half-peak width (w_p) are in the range of 113–140 mV at scan rate range of 100–1000 mV s^{-1} for the two cv waves. They are larger than that expected for the reversible electron transfer process. This is consistent with the above suggestion that, the two waves are electron transfer processes coupled with kinetic contribution.

3.3. Double potential step chronoamperometry

Chronoamperometry is used for the determination of diffusion coefficient and deduce the current nature. The double potential step chronoamperograms of 0.26 mM GA in the phosphate buffer solution (pH 1.64) are obtained at different duration times. The current of the first step, $i(t < \tau)$, is unaffected by the chemical reaction, so that it can be used to estimate the diffusion coefficient. For an electroactive material with diffusion control nature, the current corresponding to the electrochemical reaction is described by Cottrell's equation [19]:

$$i(t < \tau) = nFAD^{1/2}C^{*}_{bulk}\pi^{-1/2}t^{-1/2} \quad (5)$$

where D is the diffusion coefficient (cm^2 s^{-1}), C^{*}_{bulk} is bulk the concentration (mol L^{-1}), τ is the step duration time, n, F, and A have their usual significance. Under diffusion (mass transport) control, a plot of $i(t < \tau)$ versus $t^{-1/2}$ will be linear, and from the slope, the value of D can be obtained. A plot of $i(t < \tau)$ versus $t^{-1/2}$ gives a straight regression line, with regression coefficient value of 0.998, cf. Fig. 3, revealing that the oxidation of gallic acid is diffusion-

Table 1
Kinetic parameters for the electrochemical oxidation of 0.20 mM gallic acid at pH 1.54 and scan rate of 100 mV s^{-1}.

E_1^0 (mV/SCE)	E_2^0 (mV/SCE)	$k_1^0 \times 10^{10}$ (cm s^{-1})	α_1	$k_2^0 \times 10^7$ (cm s^{-1})	α_2	$K_1^C \times 10^7$ (s^{-1})	K_2^C (s^{-1})
99.7	368.8	3.8	0.026	1.08	0.386	83.5	3.86

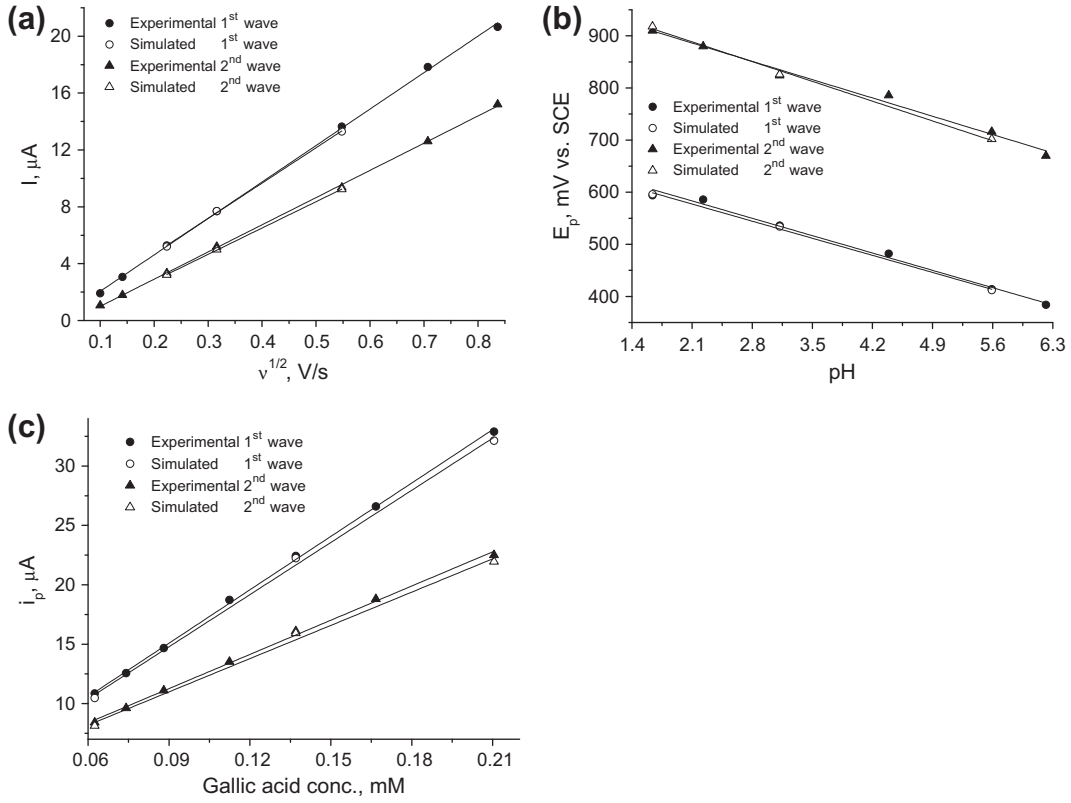

Fig. 6. Best fit of for experimental and digital simulated data at (a) different scan rates, $i_p - v^{1/2}$ plots, (b) different pH's, E_p – pH plots and (c) different substrate concentrations, i_p – [GA].

$$GA \xrightarrow{k_1^o} GA^{\bullet+} + e^-$$

$$GA^{\bullet+} \xrightarrow{k_1^f} GA^{\bullet} + H^+$$

$$GA^{\bullet} \xrightarrow{k_2^o} GA^{+} + e^-$$

$$GA^{+} \xrightarrow{K_2^b} GAO + H^+$$

Scheme 1.

controlled process over the entire range of time. The mean value of D is estimated to be 3.9×10^{-5} cm^2 s^{-1}.

3.4. Double potential step chronocoulometry

Double potential step chronocoulometry is useful technique in the determination of mechanistic pathway of electrochemical reactions and determination of diffusion coefficient. The chronocoulometric responses are represented by Eqs. (6) and (7) where Q is the amount of charge that passed at time t [19]. Chronocoulometry of 0.26 mM GA is performed in 0.4 M phosphate buffer solution (pH 1.64) at different duration times. A linear regression lines are obtained on plotting $Q(t < \tau)$ versus $t^{1/2}$ with regression coefficient of 0.998, cf. Fig. 3.

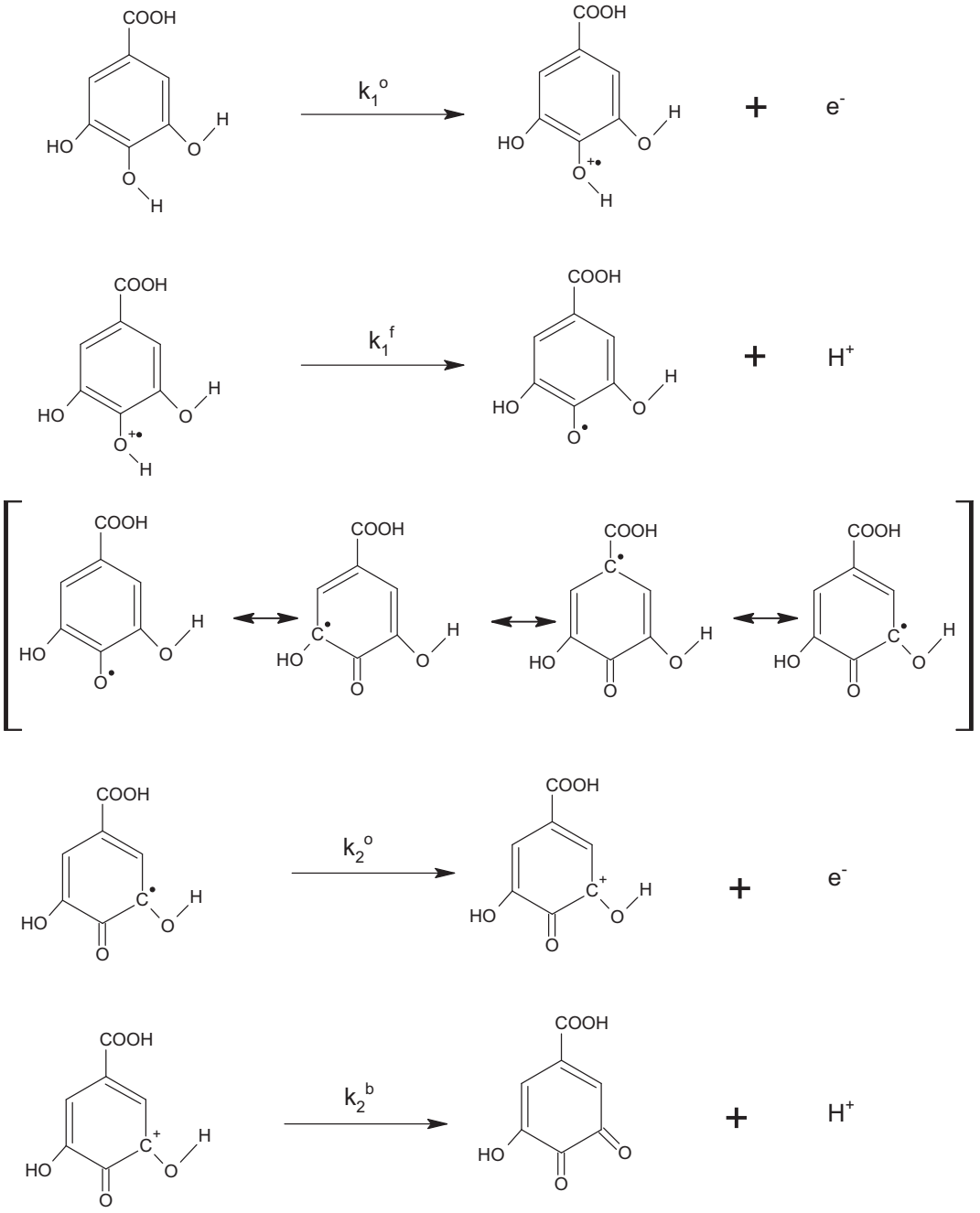

Scheme 2.

$$Q(t<\tau)=\frac{2nFAD^{1/2}C^{*}_{bulk}t^{1/2}}{\pi^{1/2}} \quad (6)$$

$$Q(t>\tau)=\frac{2nFAD^{1/2}C^{*}_{bulk}}{\pi^{1/2}}[t^{1/2}(t-\pi)^{1/2}] \quad (7)$$

Based on Eq. (6), from the (slopes of are $2nFAD^{1/2}\ C^{*}_{bulk}\pi^{1/2}$) of plots, an average diffusion coefficient of 4.0×10^{-5} cm^2 s^{-1} for GA is obtained. This value is in a good consistent with the value obtained above.

Mechanistic investigation of GA oxidation is undertaken on performing a series of double potential step experiments in which the duration time is varied over a suitable range and then comparing the experimental results to the theoretical response ratio for various mechanisms described by Hanafey et al. [20]. Chronocoulometric charge ratio, Eq. (8), is obtained from Eq. (7) at time $t = 2\tau$ and Eq. (6) at time = τ.

$$Q_R=\frac{Q_b}{Q_f}=\left[\frac{Q_{(\tau)}-Q_{(2\tau)}}{(Q_\tau)}\right] \quad (8)$$

The analysis of the chronocoulograms is done on measuring the charge ratio Q_R for a series of duration time τ and matching the Q_R versus log τ plots of the theoretical working curves that had been calculated for the different electrode ECEC mechanisms such as ECEC radical–radical dimer, ECEC parent-radical dimer and ECEC-first order [20]. On matching the experimental and theoretical curves, excellent fit is seen for ECEC, first-order mechanism, cf. Fig. 4.

3.5. Digital simulation

Digital simulation is a useful method in evaluation of complicated electrode reactions [21]. In this direction, when simulated cyclic voltammogram curves fit the experimental cyclic voltammograms, one can confirm the reaction proposed mechanism and evaluate thermodynamic and kinetic parameters for the electron transfer and chemical processes.

The experimental voltammograms are compared with the theoretical ones calculated using the DigiSim 3.03 software, in order to confirm the electrode mechanism and to estimate the kinetic parameters for the heterogeneous electron transfers and their associated chemical steps. To confirm the above deduced ECEC oxidation mechanism and obtaining the standard electrode potential, $E^{o\prime}$s, heterogeneous electron transfer rate constants, k^o, for the electrochemical processes, as well as the equilibrium constant ($K_{eq} = k_f/k_b$) values for the chemical steps, simulations are undertaken. For the diffusion coefficients, D, the default value of 4.03×10^{-5} cm^2 s^{-1} is used throughout. Different ECEC mechanisms including ECEC radical–radical dimmer; ECEC parent-radical dimmer, and ECEC first-order are tested. The transfer coefficient, α, is assumed to be 0.5, and the formal potentials are obtained experimentally from the two cv waves observed in cyclic voltammetry. The procedure is performed based on achieving the best fit between simulated and experimental cyclic voltammograms.

Fig. 5 illustrates a typical fit of simulated to experimental responses. The kinetic parameters obtained for the best fit are depicted in Table 1. The fitting procedure is carried at for different scan rates, pH's and substrate concentrations. Plots of the variation in peak current, against square root of scan rate, & in peak potentials with scan rate and dependence of peak potentials on pH are illustrated in Fig. 6. Good agreement between theoretical and experimental is obtained. Thus, the simulation using the concluded ECEC first-order mechanism agrees well with the experimental data. This reveals good evidence for the mechanism given in Scheme 1.

Recently, it was concluded that, oxidation of polyphenols can precede either by transfer of one electron via the formation of a phenoxyl radical (semiquinone) intermediate [22]. The semiquinone is unstable and decay via dimerization or polycondensation reaction. The above findings strongly suggest the exclusion of the possibility of dimerization or polycondensation reactions.

On the bases of the foregoing results, the oxidation mechanism of gallic acid is described in Scheme 1.

The first wave represents an irreversible oxidation of gallic acid (GA) to the semiquinone radical cation (GA$^{\cdot+}$) by irreversible electron transfer process. The formed radical cation loses a proton to form the semiquinone radical (GA$^{\cdot}$) [23]. The one-electron oxidation product (semiquinone radical, GA$^{\cdot}$) is followed by a second irreversible electron transfer to the quinone cation (GA^{+}). Finally, deprotonation of the quinone cation (GA^{+}) completes the overall two-electron process to give the quinone (*GAO*) which appears as an irreversible peak. The oxidation mechanism of gallic acid is described in detailed, cf. Scheme 2.

Acknowledgment

We are grateful to Dr. Ayman Nafady (University of Monach, Australia) for providing DigSim digital simulation program and useful advice.

References

[1] Z. Lu, G. Nie, P.S. Belton, H. Tang, B. Zhao, Neurochem. Int. 48 (2006) 263.
[2] O.I. Aruoma, A. Murcie, J. Butler, B. Halliwell, J. Agric. Food Chem. 41 (1993) 1880.
[3] M.W. Lee, Y.A. Lee, H.M. Park, S.H. Toh, E.J. Lee, H.D. Jang, Y.H. Kim, Arch. Pharm. Res. 23 (2000) 455.
[4] H.N. Graham, Prev. Med. 21 (1992) 334.
[5] U. Bachrach, Y.C. Wang, Amino Acids 22 (2002) 1.
[6] B.H. Kroes, A.J. van den Berg, H.C. Quarles van Ufford, H. van Dijk, R.P. Labadie, Planta Med. 58 (1992) 499.
[7] I. Kubo, P. Xiao, K. Fujita, Bioorg. Med. Chem. Lett. 11 (2001) 347.
[8] V. Novak, M. Šeruga, Š. Komorsky-Lovrić, Electroanalysis 21 (2009) 1019.
[9] Z. Yang, D. Zhang, H. Long, Y. Liu, J. Electroanal. Chem. 624 (2008) 91.
[10] S. Mu, Synthetic Metals 139 (2003) 287.
[11] S. Gunckel, P. Santander, G. Cordano, J. Ferreira, S. Munoz, L.J. Nunez-Vergara, J.A. Squella, Chem-Biol. Interact. 114 (1998) 45.
[12] P. He, L.R. Faulkner, Anal. Chem. 58 (1986) 517.
[13] S.M. Golabi, D. Nematollahi, J. Electroanal. Chem. 420 (1997) 127.
[14] S.M. Golabi, D. Nematollahi, J. Electroanal. Chem. 430 (1997) 141.
[15] D. Nematollahi, S.M. Golabi, Bull. Electrochem. 14 (1998) 97.
[16] H.R. Zare, S.M. Golabi, J. Solid State Electrochem. 4 (2000) 87.
[17] A. Bloggs, R. Cooper, D. Dobson, J.B. Gill, D.C. Goodall, B.L. Shaw, N. Taylor, T. Boddington, J. Chem. Soc. Dalton Trans. (1985) 1213.
[18] I.D. Dobson, N. Taylor, L.R.H. Tipping, Electrochemistry, Sensor and Analysis, Elsevier, Amsterdam, 1986. pp. 61–75.
[19] A.J. Bard, L.R. Faulkner, Electrochemical Methods, Fundamentals and Applications, Wiley, New York, 2001.
[20] M.K. Hanafey, R.L. Scott, T.H. Ridgway, C.N. Relley, Anal. Chem. 50 (1979) 116.
[21] M. Rudolph, D.P. Reddy, S.W. Feldberg, Anal. Chem. 66 (1994) 589A.
[22] H. Fulcrand, M. Dueñas, E. Salas, V. Cheynier, Am. J. Enol. Viticult. 57 (2006) 289.
[23] J.Q. Chambers, the Chemistry of Quinoid Compounds, in: S. Patai (Ed.), vol. 2, Wiley-Interscience, New York, 1974 (Chapter 3).